

# IMAGING FROM THE GALILEO MISSION

M.J.S. BELTON

*National Optical Astronomy Observatories  
Tucson, AZ 85716*

AND

THE GALILEO IMAGING TEAM

**Abstract.** Imaging of the Jupiter system with the Solid State Imaging (SSI) camera is discussed. The results of the experiment involve three main parts: imaging of phenomena in Jupiter's atmosphere, imaging of the Galilean satellite surfaces, and imaging of the smaller satellites and ring system.

## 1. Introduction

Imaging of the Jupiter system with the Solid State Imaging (SSI) camera (Belton et al., 1993) began on June 27, 1996, just prior to the first encounter of the Galileo spacecraft with Ganymede (G1). Imaging sequences planned for the initial approach to Jupiter in December 1995, including the first encounters with Europa and Io, were cancelled because of a technical problem with the tape recorder. Diagnosis of this problem, the development of protective operational rules for the recorder's use, and the loading of new flight software to operate the camera and return various forms of compressed and edited data were completed and fully tested during the time between Jupiter orbit insertion and G1. At the time of writing, nine orbits have been successfully completed and some 1,200 images of Jupiter and its satellites have been returned to Earth. These provide the highest spatial resolution ever achieved on Europa (22 m/pixel), Ganymede (78 m/pixel), and Callisto (125 m/pixel), i.e., a 30 times improvement over Voyager (Smith et al., 1979a,b) and up to 10,000 times better than is possible with the Hubble Space Telescope. A recently approved extension of the Galileo mission beyond December 1997 and lasting until December 1999 (the Galileo Europa mission), leaves some sixteen orbits to be accomplished (nine at Europa, five at Callisto, and two at Io). This extension should put the final SSI picture count near 3,200 and, perhaps more significantly, allow a much more expansive high spatial resolution and stereoscopic coverage of Europa. It will also include a second close encounter with Io and that should yield images of unprecedented spatial resolution (up to 6 m/pixel) on selected active volcanic regions.

The Galileo SSI camera was the first planetary imaging system to be designed with a doped-silicon CCD (800 by 800 format with 10 micron square pixels) detector system (Klaasen et al., 1984). The SSI does not have a particularly powerful telescope (angular resolution  $\sim 2$  arc-sec/pixel at F/10) but gains its remarkable spatial resolution capability from the closeness of the spacecraft encounters with the satellites (as low as 200 km above the surface). Its exceptional geologic and atmospheric diagnostic capability stems from the camera's ability to image at high angular resolution in the visible and near-infrared (0.35 – 1.0 micrometers) spectral bandpass. The camera is capable of making extended and multiple exposures that are important for imaging of Jupiter's nightside and imaging satellites in eclipse, as well as operating in its normal mode. The SSI has been fully calibrated in flight, first during the second encounter with Earth while en route to Jupiter and later during the ninth orbit around Jupiter (Klaasen et al., 1997). The calibration was found to be very stable. To make the most effective use of the limited communication capability of the spacecraft to Earth ( $\sim 100$  bits/sec on average), the SSI data (a full image is 5.12 Mbits) is usually compressed before transmission. This is accomplished by either lossy or lossless compression algorithms or by

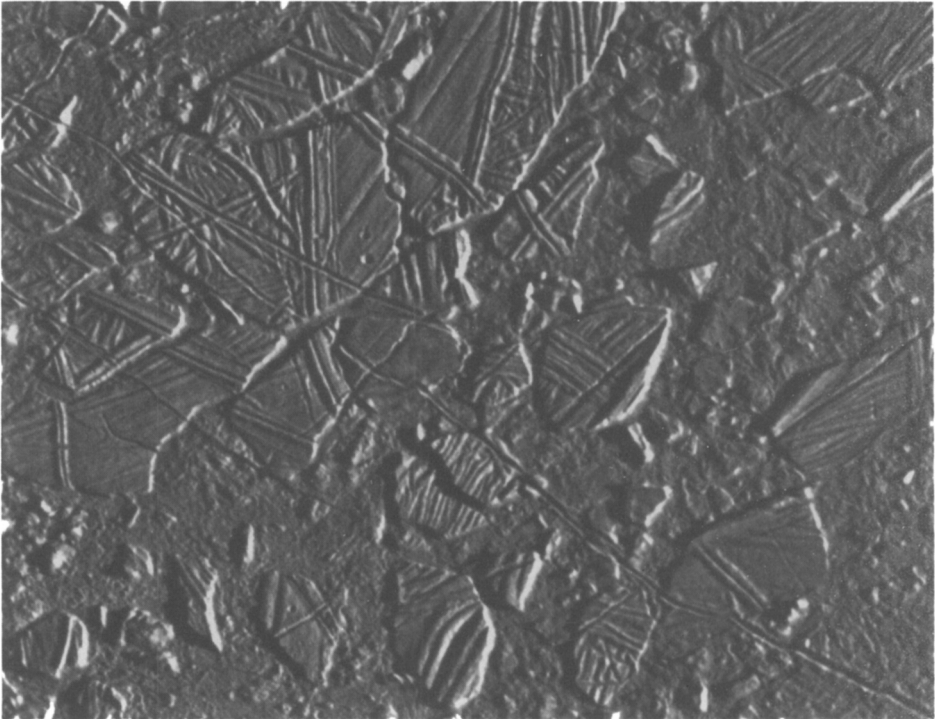


*Figure 6.* Ice rafting on Europa. This very high-resolution picture, taken through the clear filter, represents a small area (32 by 42 km) in a region called Connemara. The small plates seem to have broken away from the periphery of the area and have drifted, rotated, and, in some cases, tilted in much the same way that ice floes behave in terrestrial icepacks. It is thought that the material between the small plates was either melted or extremely ductile at some, as yet undetermined, time in the past.

editing the size of the returned image. Sometimes very heavily compressed images (20:1 or greater) are returned simply to locate small features of interest in the image. A limited region around such a feature is then returned on a second pass through the tape with lossless compression. Typically satellite images are compressed by a factor of  $\sim 6:1$  and atmospheric images by  $\sim 10:1$ .

For operational purposes the SSI imaging experiment divides into three distinct parts (Belton et al., 1993): imaging of phenomena in Jupiter's atmosphere, imaging of the Galilean satellite surfaces (Carr et al., 1995), and imaging of the smaller satellites and ring system.

## 2. Jupiter's Atmosphere

The ability of the SSI camera to accomplish high spatial resolution imaging (typically 12 km/pixel on Jupiter) at near-infrared wavelengths is the key to the Galileo atmospheric experiment. Band-passes around 727, 756, and 889 nanometers allow quantitative characterization of the local strength

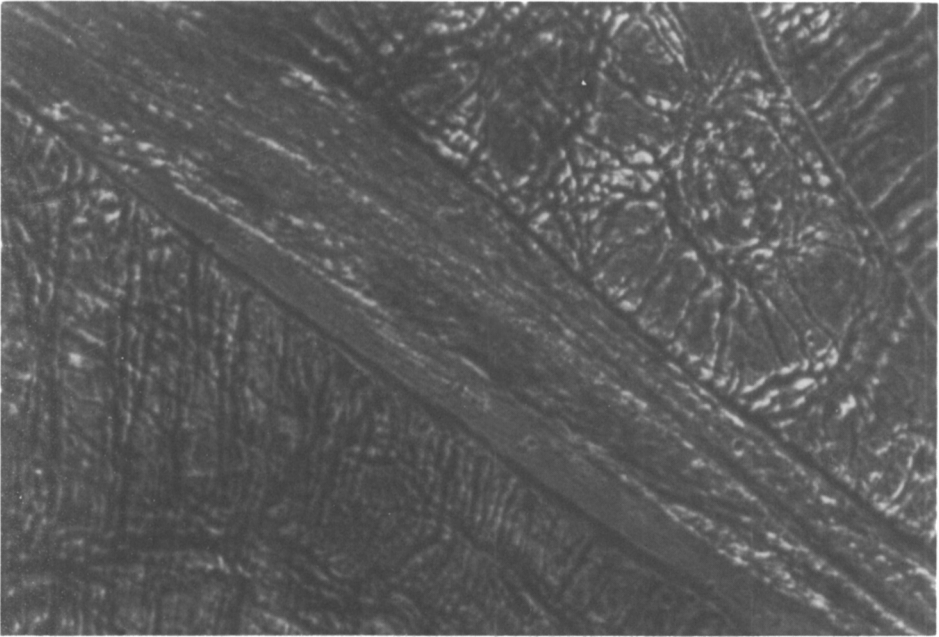


*Figure 7.* Fractured dark terrain on Ganymede. This 200 m/pixel image was taken through the clear filter during the Ganymede 8 encounter. It shows an example of the tectonic disruption that has occurred on the surface of this satellite. Surprisingly, there are few indications of any accompanying volcanic activity.

of methane absorption over specific atmospheric features (Fig. 1, see color plates). These spectral measurements are coupled with imaging of the same feature under different illumination conditions and time-lapse sampling to yield the vertical cloud structures associated with the feature and an estimate of the shear of the wind field both horizontally and vertically. Coupled with information on the vertical structure of the gaseous part of the atmosphere obtained by the near-infrared mapping spectrometer (NIMS) (Carlson et al., 1996), these data will tell us much about the dynamical nature of these features. So far data on the Great Red Spot, a typical white oval, and two analogs of the Galileo Probe descent region (5-micron hotspots) have been collected (Belton et al., 1996). In the latter case, NIMS and SSI observations have been essential elements in arriving at a rational explanation for the very low and enigmatic measurements of water content that were made by the Galileo probe mass-spectrometer (Niemann et al., 1996). Observations by the NIMS instrument have shown enormous deficiencies of water content in the center of hotspots relative to surrounding areas, and SSI has shown the region to be the center of a strong atmospheric downdraft and relatively devoid of clouds. Galileo imaging of the planet is not restricted to observations of the daylit clouds. Observations have also been made of the northern auroral oval, the thumbprint of Jupiter's magnetosphere on the planet's atmosphere (Fig. 2, see color plates). Future acquisition of data on the distribution of lightning strokes and phenomena occurring at the intersection of Io's flux tube with Jupiter's atmosphere are planned for the upcoming Callisto 10 encounter.

### 3. The Galilean Satellites

The most exciting part of the SSI observations of Io are still in the future and should happen during the final two orbits of the Galileo Europa mission in 1999 when surface resolutions obtained for Io may reach as high as 6 m/pixel. During the primary mission the highest resolution that has been achieved is about 2.6 km/pixel. While this is substantially less than the best resolution achieved by Voyager (Smith et al., 1979a,b), the SSI's ability to image into the near-infrared, coupled with the two-year observing period and the 100 times improved sensitivity of the Galileo CCD detector,

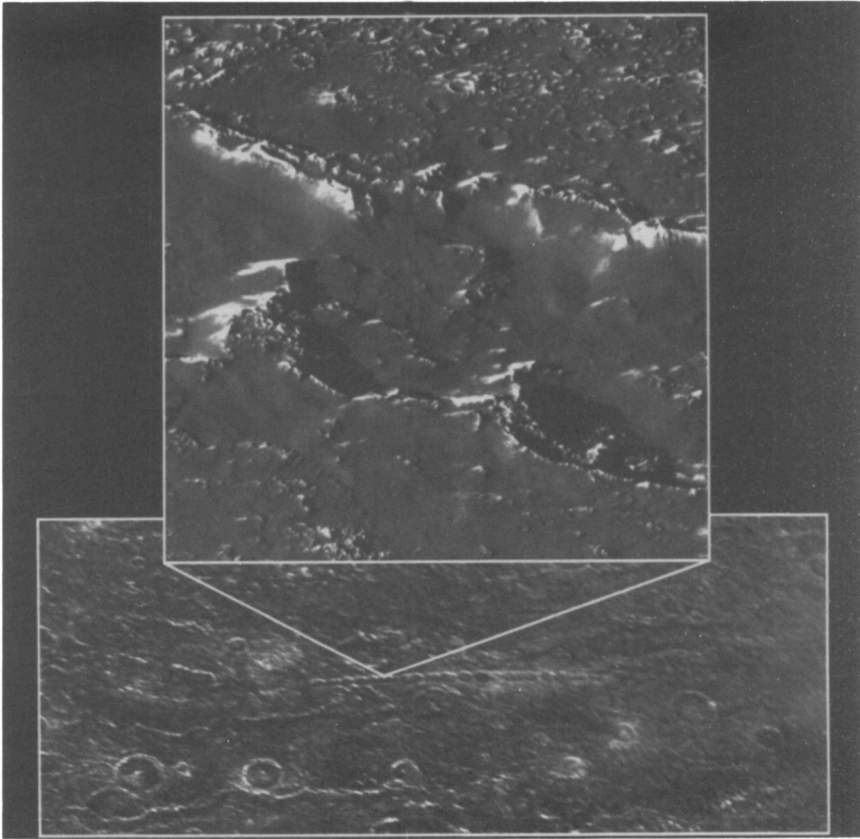


*Figure 8.* Part of a catena (or string of craters) probably caused by the impact of a fractured comet nucleus on Callisto. Note the dearth of small craters and the apparently ubiquitous covering of dark material. This image was taken on the Callisto 3 encounter. In the upper part the resolution is 38 m/pixel and the area covered is only about 13 by 13 km.

has brought a host of new results. Imaging of volcanic hotspots in Jupiter eclipse (Fig. 3, see color plates) has shown that many of these features are much hotter (up to 1800 K) and smaller than previously thought (McEwen et al., 1997). Siliceous volcanism is clearly involved. Eclipse images have also allowed the distribution of the tenuous atmosphere to be mapped out as it glows (Io-glow) under impact from energetic magnetospheric particles. Monitoring of surface phenomena (Fig. 4, see color plates) and of plume activity has clearly shown how changes in color, photometric properties, and frequency can occur as volcanic activity changes. There is a good case for high-temperature stealth plumes (Johnson et al., 1995) in the data.

At Europa, which was the satellite with the poorest high-resolution coverage by Voyager, the images (Figs. 5 [see color plates] and 6) point solidly to the presence of a global ocean a few kilometers below the icy surface at sometime in its past history (Carr et al., 1997). The paucity of impact craters on Europa's surface intuitively implies that the surface is geologically very young — however, this is not rigorous and model-surface age estimates currently run from a few million to billions of years. To resolve this problem, future observations from Galileo will include searches for present-day cryo-volcanic activity and for physical constraints on the surface age.

At Ganymede the prime SSI objective was to determine the physical origins of the bright, lineated (sulci) and the dark (regio) terrains. It was anticipated that some kind of volcanic activity (e.g., large-scale resurfacing in the bright regions) might be the cause. This has not turned out to

be the case and essentially all of what is seen (Fig. 7) on the surface is due to tectonic activity and to impact cratering (Collins et al., 1997).

Callisto has provided many surprises. This satellite was anticipated to have a very old surface saturated by small impact craters over an undifferentiated interior and therefore to be of the least geologic interest. The SSI images have revealed a surface surprisingly deficient in small craters (Fig. 8). There are clear signs of widespread degradation of crater rims due to sublimation, particle erosion, or some other unknown process evident everywhere. The entire landscape is apparently draped with a thick layer of mobile dark material, again of unknown origin.

#### 4. Small Satellites and Jupiter's Ring System

Galileo's orbit is providing many excellent opportunities to observe Jupiter's non-Galilean satellites, particularly Amalthea, Adrastea, Metis, Thebe, and the ring system (Fig. 9, see color plates). New data has been obtained on the main and gossamer rings and the ring halo. Even though the orbit of Galileo constrains our observations of the ring to very small inclination angles (approximately 0.5 degrees in the Callisto 3 orbit), both radial and azimuthal structures have been observed in the ring ansae.

#### 5. Conclusion

The mission of Galileo at Jupiter is not yet half over. Many exciting discoveries have been made, particularly in the cases of the satellites Europa and Io. These satellites are now the focus of the two-year extension of the Jupiter mission into the Galileo Europa Mission. We expect to more than double the imaging coverage of Europa that was originally planned, with emphasis on very high-resolution geologic studies, stereography of topographic features, a search for active cryo-volcanic plumes, and color work. At Io the focus will shift from a moderate-resolution plume and surface monitoring experiment to detailed studies of active plume vents and hotspots at very high spatial resolution (up to 6 m/pixel) as the spacecraft swoops down to within 300 km of the satellite's tortured surface.

#### Acknowledgements

The Galileo Imaging Team would like to acknowledge the support and continual encouragement given to it by the Solar System Exploration Program at NASA Headquarters under the leadership of the late Dr. J. Rahe.

#### References

- Belton, M.J.S. et al. (1996) *Science*, **274**, pp. 377–384.
- Belton, M.J.S. et al. (1993) *Space Sci. Rev.*, **60**, pp. 413–455.
- Carlson, R. et al. (1996) *Science*, **274**, pp. 385–388.
- Carr, M.H. et al. (1995) *J. Geophys. Res.*, **100**, pp. 18935–18955.
- Carr, M.H. et al. (1997) *Nature*, (submitted).
- Collins, G.C. et al. (1997) *Geophys. Res. Lett.*, (submitted).
- Johnson, T.V. et al. (1995) *Geophys. Res. Lett.*, **22**, pp. 3293–3296.
- Klaasen, K.P. et al. (1984) *Opt. Eng.*, **23**, No. 3, pp. 334–342.
- Klaasen, K.P. et al. (1997) *Opt. Eng.*, **36**, (in press).
- McEwen, A.S. et al. (1997) *Geophys. Res. Lett.*, (in press).
- Niemann, H. et al. (1996) *Science*, **272**, pp. 846–840.
- Smith, B.A. et al. (1979a) *Science*, **204**, pp. 951–972.
- Smith, B.A. et al. (1979b) *Science*, **206**, pp. 927–950.